Spatial Robustness Analysis of a Single-Lead ECG Algorithm for Breathing Rate Estimation

Amaël Mombereau[1], Vladimír Sobota[1], Carmen Martinez Anton[1], Rémi Dubois[1], Michel Haissaguerre[1,2], Kanchan Kulkarni[1*], Laura R Bear[1*]

[1]Université de Bordeaux, INSERM, CRCTB, U 1045, IHU Liryc, Bordeaux, France
[2]Department of Electrophysiology and Cardiac Stimulation, Centre Hospitalier Universitaire de Bordeaux, Bordeaux, France
*These authors contributed equally as last authors

Abstract

Breathing rate (BR) is a vital physiological parameter increasingly used for patient monitoring. Traditional BR sensors are often unsuitable for wearable or dense ECG applications. We evaluated the spatial robustness of an open-source algorithm for BR estimation from single-lead ECG using a high-density dataset from 40 healthy adults with a 118-electrode thoracic array. Unlike previous studies, we assessed performance not only per electrode but also for all possible electrode pairs, considering one electrode as a fixed reference. BR was estimated for each pair and compared to a plethysmographic reference. When the reference electrode is positioned in the upper central thorax, pairing with electrodes located diagonally or laterally to the left consistently yields the lowest median Mean Absolute Error (1.82 [1.45-2.28] bpm). Conversely, pairings toward the right or inferior right thorax tend to degrade performance. These findings demonstrate that both electrode location and pairing geometry strongly influence BR estimation accuracy, suggesting that optimized asymmetric placement could enhance performance in wearable systems.

1. Introduction

Breathing rate (BR) is a fundamental vital sign, routinely measured in clinical practice to assess patient status and detect early signs of deterioration. Despite its clinical relevance, BR is often measured sporadically rather than continuously, mainly due to limitations in existing monitoring technologies. Conventional systems such as respiratory belts, nasal thermistors, or impedance pneumography can be cumbersome, intrusive, or susceptible to motion artefacts, making them less suitable for long-term or ambulatory use.

In recent years, algorithms capable of estimating BR from electrocardiogram (ECG) signals have emerged as an attractive alternative. ECG-derived respiration (EDR) leverages subtle respiratory-related modulations in the ECG signal, such as baseline wander, QRS axis rotation, and amplitude changes, to estimate BR without requiring additional sensors. This approach offers a contact-based, unobtrusive alternative that is well suited for wearable monitoring. Among these, Kulkarni et al. introduced an open-source, single-lead ECG algorithm that combines time- and frequency-domain processing [1]. This method demonstrated promising accuracy in both human and animal studies, highlighting its potential for wearable applications.

In wearable or high-density ECG systems, electrode placement may be dictated by device requirement or patient-specific constraints, potentially affecting the strength of respiratory modulation and, consequently, BR estimation accuracy. While some studies have examined optimal electrode locations for general ECG quality or cardiac parameter extraction, the spatial robustness of EDR algorithms, i.e., their ability to maintain accuracy across varying electrode positions, remains underexplored. That is, most prior work has focused on single or limited electrode configurations, often corresponding to standard 12-lead ECG positions due to constraints in data collection/availability.

In this study, we investigate the spatial robustness of the Kulkarni et al. single-lead EDR algorithm using high-density (128 electrode) ECG recordings from healthy adults [1]. Such a dense electrode array provides a unique opportunity to map spatial variability, enabling a detailed assessment of how electrode position influences EDR performance. We quantify BR estimation accuracy across all electrode positions and pairings, compare spatial patterns to known optimal ECG locations, and analyze the influence of inter-electrode distance and orientation on performance. This knowledge is essential for guiding electrode placement in future wearable devices, where optimizing both signal quality and respiratory sensitivity could significantly improve monitoring reliability.

2. Methods

ECG data were collected from 40 healthy adult volunteers (age 45 ± 16.4 years, 54% male). The study was approved by local ethics committee and all volunteers gave informed consent. A 128-electrode BioSemi system was used with electrodes covering the chest (Figure 1). The single electrode band positioned near the spine has not been used. Signals were sampled at 2048 Hz and pre-processed with a Butterworth band-pass filter (0.5–250 Hz) and a 50 Hz notch filter to remove noise and baseline wander. Ground-truth respiratory signals were simultaneously acquired using a plethysmography belt connected to the same BioSemi acquisition system. The raw respiratory signal was further processed with *NeuroKit2*'s rsp_clean function to remove artifacts, and respiratory peaks (inspiration onsets) were detected using *rsp_findpeaks*. Instantaneous BR was then computed from consecutive inter-peak intervals as

$$BR[n] = \frac{60 \times fs}{RSP\_Peaks[n+1] - RSP\_Peaks[n]}$$

where fs=2048 Hz is the sampling frequency and RSP_Peaks are the detected inspiration indices. This produced a breath-by-breath series of BR.

BR was estimated from each electrode's ECG signal using a Python-based open-source algorithm developed for BR estimation from single-lead ECG signals and described in detailed in [1]. In brief, the algorithm computes the root mean square (RMS) amplitude of each QRS complex in a moving 16-beat window, and then applies a fast Fourier transform to the RMS signal to extract the dominant respiratory frequency. This method combines time- and frequency-domain features to estimate BR.

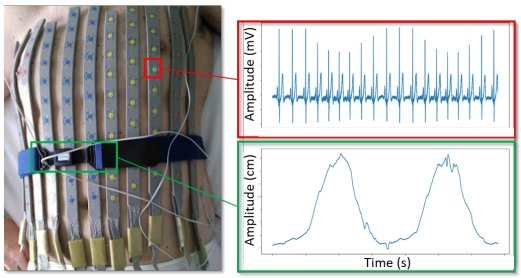

Figure 1: BioSemi 128-electrode thoracic array with example single-lead ECG (red) and reference respiratory signal (green).

The algorithm was applied to 13,806 bipolar signals per volunteer, obtained by pairing each reference electrode (118 in total) with the remaining 117 electrodes on the BioSemi grid.

Estimated and reference BR were compared using the mean absolute error (MAE) in breaths per minute (bpm) for each volunteers' recordings (10 ± 2 mins each) and for each bipole. Spatial analysis of MAE values was performed to assess the robustness of the algorithm across different electrode positions. Comparisons were made between traditional precordial regions and alternative locations, such as the right lateral thorax. Results are reported as median and interquartile range [Q1-Q3].

3. Results

3.1. Impact of Relative Orientation on BR Estimation Accuracy

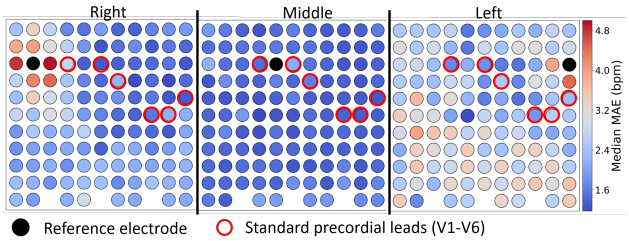

Figure 2: Median MAE maps for BR estimation. Each map shows median error for one reference electrode (black) paired with all others over all the patients. Standard precordial positions (V1–V6) are highlighted in red.

The spatial distribution of median MAE values across all patients demonstrated a clear dependence on electrode orientation. For reference electrodes located in the upper or central thorax, pairings with electrodes oriented to the right and inferior-right consistently produced lower MAE values (≈ 2.0 bpm, dark blue), while pairings toward the left yielded substantially higher errors (up to ≈ 4.5 bpm, red). This directional pattern was reproducible across different reference electrodes, as illustrated in Figure 2, where the reference electrode is shown in black and the standard precordial leads V1–V6 in yellow.

Quantitative analysis of angle and distance confirmed these observations. Figure 3.A and B show that median MAE values varied significantly with electrode pair orientation: lefttward orientations (0°–90° and 270°–360°) yielded lower errors (median MAE = 1.82 [1.45-2.28] bpm) than rightward orientations (90°–270°; median MAE = 2.4 [1.9-3] bpm, $p < 0.0001$). No significant difference was respectively observed between downward (270°–360°, 180°–270°) and upward (0°–90°, 90°–180°) orientations, although slightly lower values were generally found around 0°–90°. The polar representation confirmed these angular trends, with minimal MAE values concentrated in the right and inferior-right quadrants of the reference electrode.

Figure 3.C shows the variation of median MAE as a function of electrode separation distance, for left-sided (green) and right-sided (orange) pairings.

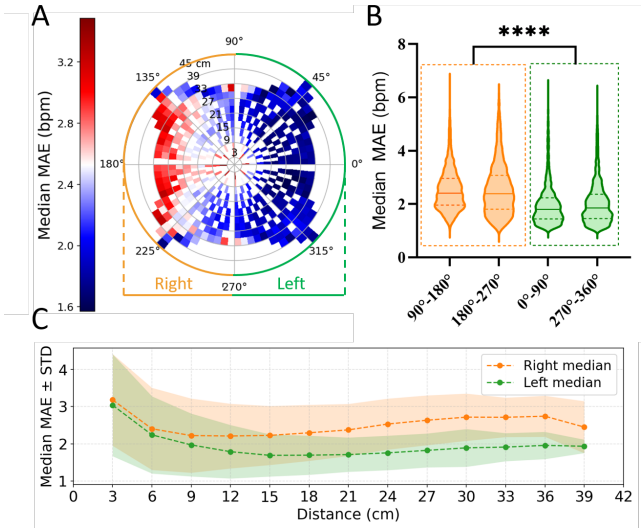

Figure 3: BR estimation accuracy as a function of electrode pair geometry. A. Polar map of MAE by angle and distance. B. Violin plots of median MAE across angular sectors. C. Median MAE versus inter-electrode distance. **** $p < 0.0001$.

In both cases, MAE decreased sharply within the first 6–9 cm. Beyond this range, performance tended to stabilize, but the trend differed between sides: for right-sided pairings, MAE reached a stable level after ~6 cm and showed little further change, while for left-sided pairings, MAE continued to decrease more gradually. At greater distances, the error stabilised, although the most distant points were less reliable due to the reduced number of electrode pairs.

3.2. Identification of High-Performance Electrode Regions

The mean of median MAE values across all patients for each reference electrode is shown in Figure 4.A. Performance varied across the thorax, with the lowest values concentrated in the central–upper regions (≈1.21–1.79 bpm), particularly in areas 2 and 6.

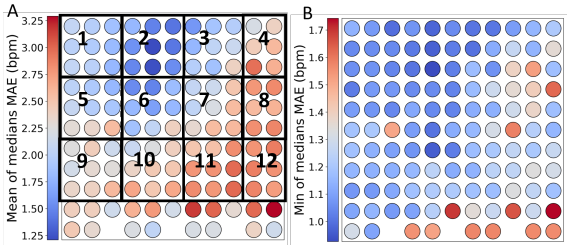

Figure 4: Spatial distribution of mean and minimum median MAE values per reference electrode. (A) Mean of median MAE values across all patients. The electrode grid is divided into predefined anatomical areas (1–12). (B) Minimum of median MAE values across all patients.

In contrast, higher errors were observed in the inferior and lateral left zone, with mean median MAE values reaching up to 3.29 bpm (area 12).

The minimum of median MAE values for each reference electrode (Figure 4.B) further highlighted these trends. Several electrodes in the upper and central thorax achieved minimum median MAE values close to 1.0 bpm, while even the least favorable electrodes rarely exceeded 1.7 bpm. This confirms that although overall performance depends on electrode location, all regions of the thorax were capable of providing accurate estimates under optimal pairings.

The heatmap (Figure 5.A) shows the mean of median MAE values between all combinations of reference and paired zones. Performance was not uniform across the thorax. The lowest errors were consistently observed when electrodes from area 2 were used as reference and paired with area 3 (1.24 bpm). In contrast, higher errors occurred when involving areas 7, 8, 9, 10, or 12, with mean median MAE values exceeding 4 bpm in several cases (e.g., area 7–area 1: 4.33 bpm; area 12–area 12: 4.56 bpm).

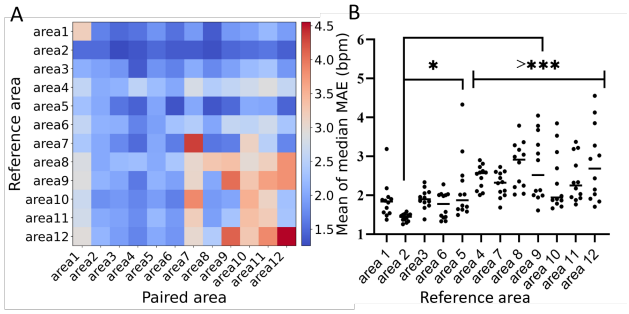

Figure 5: Comparison of median MAE across electrode area. (A) MAE values for BR estimation across all patients, computed between reference electrodes and paired electrodes grouped by anatomical areas. (B) Distribution of mean median MAE values for each area. Statistics: Friedman test. *p<0.05, ***p<0.001.

The distribution of mean median MAE values per area (Figure 5.B) further highlights these differences. Areas 2 and 6 yielded the most accurate and stable results (≈ 1.5–2.3 bpm), significantly outperforming inferior and lateral zones such as areas 8, 9, 10, and 12, where errors often exceeded 3 bpm ($p < 0.05$, $^{**}p < 0.001$).

4. Discussion

This study investigated the spatial robustness of an open-source EDR algorithm applied to high-density thoracic recordings. Our results highlight that both electrode and reference location and the relative orientations play a crucial role in BR estimation accuracy. We demonstrated that the overall performance of the algorithm was satisfactory across the torso. However, large spatial variations were observed. Reference electrodes

located in the upper-central thorax, above precordial leads V1–V4**,** yielded the lowest median MAE values, while inferior and left-lateral regions performed substantially worse. These findings are consistent with previous work on optimized ECG electrode positioning for signal quality [2], and indicate that the upper-central thorax provides the most favorable geometry for capturing respiratory-related ECG modulation.

When evaluating all possible electrode pairs, relative orientation emerged as the dominant factor. Pairings on the right side of the thorax and in the inferior-right quadrant consistently minimized MAE while left-sided pairings produced significantly higher errors. No significant difference was observed between upward and downward orientations, although slightly better values were found in the 0°–90° sector. In contrast, inter-electrode distance had a limited effect: performance improved rapidly within the first 6–9 cm of separation, and showed little further change beyond this range.

The zone-based analysis (Figure 5) confirmed the existence of high-performance electrode regions. The upper-central thorax, used as the reference electrode area consistently outperformed all other regions and showed higher robustness to pair orientation. In contrast, zones located inferiorly or laterally (areas 8–12) produced the highest errors, and were more sensitive to orientation. Notably, the best-performance was obtained by pairing areas 2 and 3, corresponding to electrodes located above V1-V2 and V3-V4.

Mechanistically, the spatial asymmetry can be explained by several interacting factors. In regions with low MAE, respiratory modulation of QRS amplitude is strong, producing clear oscillations in the RMS signal and a dominant respiratory peak in the frequency spectrum. In the areas with high MAE, the modulation is weaker, and the respiratory peak may be overshadowed by noise or motion artefacts. Despite data selection based on signal quality, it was not possible to fully control for subject movements or speech during recordings, which may also have contributed to spurious peaks and degraded accuracy [3-4]. In addition, the algorithm is highly sensitive to R-peak detection: small errors or inconsistencies in detecting R-peaks directly affect QRS segmentation and RMS computation, which in turn propagate to the spectral analysis stage. We also observed that the polarity of the bipolar lead appeared to influence this method, suggesting that lead orientation and sign convention can further impact the robustness of BR estimation. Together, these factors explain why some electrode regions yield consistently more reliable estimates than others.

These findings have practical implications for wearable device design. Traditional used precordial positions, while optimized for cardiac diagnosis, are not necessarily ideal for EDR monitoring. Instead, our results suggest positioning the reference electrode in the upper-central thorax and with an electrode on the left or inferior-left thorax will maximize BR accuracy. Such asymmetric, geometry-driven placement strategies could enhance robustness in ambulatory monitoring, where electrode positioning is often constrained.

5. Conclusion

This study confirms the feasibility of single-lead ECG-based BR estimation using a high-density electrode layout. It reveals that the performance of the algorithm by Kulkarni et al. is spatially dependent, with some regions offering more reliable estimates than others. These insights are relevant for the design of future wearable BR monitors and argue for careful electrode placement beyond traditional ECG configurations.

Acknowledgments

The authors would like to thank the nurses and engineers without whom the volunteer dataset could not have been acquired. We would also like to thank the previous authors of the EDR algorithm used in this study for making their code available. Finally, this research was financially supported by the National Research Agency (ANR-10-IAHU-04), the ANR JCJC TUNE (ANR-22-CE17-0023), and the IHU-Liryc Internal Call (RASE).

References

[1] J. D. Roberts, R. D. Walton, V. Loyer, O. Bernus, et K. Kulkarni, « Open-Source Software for Respiratory Rate Estimation Using Single-Lead Electrocardiograms », *Sci. Rep.*, vol. 14, nº 1, p. 167, janv. 2024, doi: 10.1038/s41598-023-50470-0.

[2] H. Zhu, Y. Pan, F. Wu, et R. Huan, « Optimized Electrode Locations for Wearable Single-Lead ECG Monitoring Devices: A Case Study Using WFEES Modules Based on the LANS Method », *Sensors*, vol. 19, nº 20, p. 4458, oct. 2019, doi: 10.3390/s19204458.

[3] C. Varon *et al.*, « A Comparative Study of ECG-derived Respiration in Ambulatory Monitoring using the Single-lead ECG », *Sci. Rep.*, vol. 10, nº 1, p. 5704, mars 2020, doi: 10.1038/s41598-020-62624-5.

[4] J. Sola-Soler et B. F. Giraldo, « Comparison of ECG-Derived Respiration Estimation Methods on Healthy Subjects in function of Recording Site and Subject Position and Gender », in *2020 42nd Annual International Conference of the IEEE Engineering in Medicine & Biology Society (EMBC)*, Montreal, QC, Canada: IEEE, juill. 2020, p. 2650-2653. doi: 10.1109/EMBC44109.2020.9176438.

Address for correspondence:

Amaël Mombereau
Av. du Haut Lévêque, 33600 Pessac
Amael.mombereau@ihu-liryc.fr